Single-exciton energy shell structure in InAs/GaAs quantum dots

S. Awirothananon,[1] S. Raymond,[2] S. Studenikin,[2] M. Vachon,[1,2] W. Render,[2] A. Sachrajda,[2] X. Wu,[2] A. Babinski,[3] M. Potemski,[4] S. Fafard,[1] S. J. Cheng,[5] M. Korkusinski,[2] and P. Hawrylak[2]

[1]*Department of Physics, University of Ottawa, Ottawa, Ontario, Canada K1N 6N5*

[2]*Institute for Microstructural Sciences, National Research Council of Canada, Ottawa, Ontario, Canada K1A 0R6*

[3]*Institute of Experimental Physics, Warsaw University, Hoza 69, 00-681 Warsaw, Poland*

[4]*Grenoble High Magnetic Field Laboratory, CNRS, BP 166, 38042 Grenoble Cedex 9, France*

[5]*Department of Electrophysics, National Chiao Tung University, Hsinchu, 30050 Taiwan, Republic of China*

(Received 31 July 2008; published 22 December 2008)

The energy shell structure of a single exciton confined in a self-assembled quantum dot (QD), including excited states, is studied in a regime where the direct Coulomb attraction energy is comparable to the kinetic energy of the carriers. This is achieved via magnetophotoluminescence excitation spectroscopy experiments, where a magnetic field applied perpendicular to the plane of the QD is used to reveal the angular-momentum content of energy shells. The absorption spectrum of the QDs is modeled, and comparison with experiment allows us to relate the observed transitions to interband QD bound-state transitions. The blueshift of the absorption peaks compared to the emission peaks is then interpreted in terms of many-body interactions, and we show that for a highly symmetric situation, the observed energy difference gives a direct measurement of the extra exchange energy gained upon addition of an extra exciton in the QD.

DOI: 10.1103/PhysRevB.78.235313 PACS number(s): 78.55.Cr, 78.67.Hc, 73.21.La, 75.75.+a

I. INTRODUCTION

Quantum dot (QD) systems have established themselves as prime candidates for implementing many applications. For some applications, such as lasers,[1] superluminescent diodes,[2] and semiconductor optical amplifiers,[3] the device operation is likely to make direct use of the QD excited states. For other applications, such as single-photon source,[4] optical quantum gate,[5] and spin memory,[6] the QD contains at most two excitons at a time and only the ground state (GS) is directly involved. However, it has been shown that the presence of excited states, through configuration mixing, will influence the energy shell structure of all bound states, including the ground state.[7] Simply put, maximizing the application potential of QD systems requires understanding and modeling their energy shell structure, including the excited states, as precisely as possible.

Magnetoluminescence experiments are a technique of choice to probe QD excited-state energy shell structure, where applying an external magnetic field reveals the relevant energy shell structure by progressively lifting degeneracies and shifting the transitions associated with different angular-momentum channels as the field is increased. For example, in a series of recent experiments, it was shown that the energy shell structure of an interacting ensemble of carriers confined in QDs is that of Fock-Darwin (FD) states.[8] This was demonstrated for electron droplets using transport and resonant tunneling spectroscopy,[9,10] electron-hole (e-h) droplets (or excitonic droplets) using optical spectroscopy, and more precisely magnetophotoluminescence (MPL).[11–13] In the latter case, the relevant quasiparticle is a charge-neutral exciton, or more precisely a QD exciton. Adding many such QD excitons in a QD creates an excitonic droplet, i.e., an ensemble of interacting electron-hole pairs confined in a particular QD. Due to fast relaxation of the droplet into its ground state (GS) configuration,[14] one must fill the lower-energy shells before the excited-state emission can be observed. As a result, many relevant carrier-carrier interactions must be included to describe the system, such as Coulomb repulsion, Coulomb attraction, and exchange and correlations. This is a rather complex problem, and it is therefore desirable to perform experiments which probe the single-exciton energy shell structure of the QD bound states. Such data could be used as a stepping stone to validate theoretical models, and also the information thus gained would be directly relevant to certain applications.

This can be achieved via absorption experiments where resonant optical excitation creates excitons one by one in an excited state of an empty QD. However, in view of the small absorption cross section of QDs, such experiments are not straightforward to implement, especially in high-magnetic-field apparatus where space is very limited. Moreover, most MPL experiments published in the literature deal with QD ensembles, and it is desirable to limit the effects of inhomogeneous broadening. In photoluminescence (PL) excitation (PLE) spectroscopy, one sets the detection energy over a narrow range within the GS transition and uses resonant optical excitation to create excitons one by one in an excited state of an empty QD.[15,16] By sweeping the excitation energy, one can trace variations in the GS signal and reconstruct the equivalent of an absorption spectrum. Moreover, by selecting a subset of the QD ensemble when using a narrow detection range, one reduces the effects of inhomogeneous broadening. Very few magnetophotoluminescence excitation (MPLE) studies can be found in the literature.[17–21] Only one was performed on a sample with well-resolved excited-state emission but that study observed only the *p*-shell absorption, and it was limited to 14 T.[17]

Here, we present MPLE results up to 28 T, where *p*- and *d*-shell absorption as well as a number of weaker "indirect" transitions are observed. Experimental spectra are compared to detailed theoretical modeling, and all the transitions observed in the spectra are reproduced by our model, including their magnetic-field dependence, which allows their unambiguous assignment. Thus, a detailed description of the single-excitonic energy shell structure in self-assembled

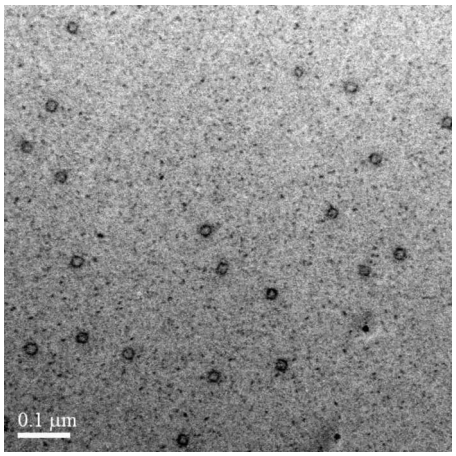

FIG. 1. Zone axis (001) bright field plan-view STEM image of an as-grown piece of the QD sample used in this study. The QD areal density obtained is $5 \pm 1 \times 10^9$ cm^{-2}, while the QD diameter is ~20 nm.

quantum dots is obtained. Finally, a blueshift of the PLE peaks as compared to the PL peaks is shown to give an estimate of the magnitude of exchange energies for excitonic droplets bound in QDs.

II. EXPERIMENT

The original wafer consists of a single layer of InAs QDs grown by molecular-beam epitaxy on *n*-doped GaAs substrate in the Stranski-Krastanow growth mode. After deposition of a GaAs buffer, 1.9 ML of InAs was deposited at 515 °C, followed by an *in situ* anneal of 60 s, and an In-flush procedure applied after deposition of 5.0 nm of GaAs.[22] The sample was terminated with the growth of a 100 nm GaAs cap. Figure 1 presents a typical plan-view scanning transmission electron microscope (STEM) image of the QD layer where it can be seen that a sparse ensemble of randomly positioned QDs is obtained. Averaging over many areas similar to that presented on Fig. 1, we obtain a QD density of 5.0×10^9 cm^{-2}, with an average lateral diameter of 20 nm. From growth conditions, the QD height is estimated to lie in the range of ~3–3.5 nm.

After growth, the wafer was cleaved into 5×5 mm^2 pieces before rapid thermal annealing (RTA) was performed. Our piece of interest was annealed for 30 s at a temperature of 825 °C using a GaAs proximity cap to stabilize the sample surface. The RTA procedure blueshifts the QD emission and decreases the shell energy spacing as well as the inhomogeneous broadening. These effects are beneficial for MPLE experiments, where the blueshift sets the signal in the tunability range of our excitation source, the reduced energy spacing facilitates the observation of transition crossings at lower magnetic fields, and the reduced inhomogeneous broadening helps improve the precision of the results.[23]

The sample was mounted on a probe at the tip of an insertion rod, which allowed the sample to be lowered into a cylindrical liquid-helium cryostat, which itself could be inserted into the bore of a suitable magnet, thus allowing the

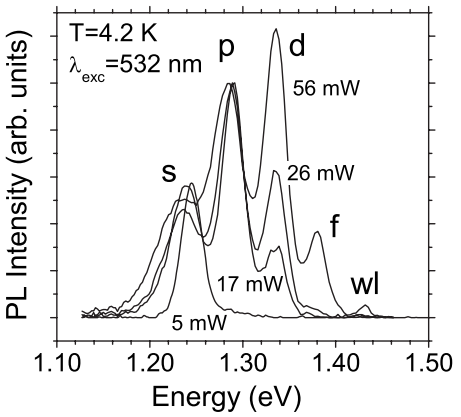

FIG. 2. Power dependence of the QD ensemble photoluminescence revealing emission from *s*, *p*, *d*, and *f* shells. The emission intensity of higher-energy shells increases with excitation power.

sample to be subjected to high magnetic fields while being kept at liquid-helium temperature (4.2 K). Three different experimental configurations were used to effect the measurements. The first two configurations made use of an 18 T Oxford superconductive magnet. For MPL measurements, a single 50-μm-core-diameter multimode optical fiber was used. The as-cleaved fiber was placed just above the sample surface, with the fiber oriented along the surface normal. The 532 nm line obtained from a Nd:YVO_4 laser was used to excite the sample surface, while the ensuing infrared signal from the QDs was collected via the same fiber and coupled to the entrance slits of a double-grating monochromator with a resolution of ~1 meV. The output optical signal of the spectrometer was detected via a liquid-nitrogen-cooled Ge detector, and the resulting signal was recorded using standard lock-in techniques. For MPLE measurements, a dual fiber probe arrangement was used where the wavelength tunable output of a Ti:Sapphire laser was coupled into the launch fiber which was tilted with respect to the sample surface normal, while the resulting QD signal was collected via a second fiber oriented parallel to the sample normal. This arrangement was used to minimize the laser back reflection into the collection fiber. Signal recording was achieved as described above for the MPL.

The third configuration was used to effect MPLE measurements up to 28 T. In this case, a resistive magnet at the Grenoble High Magnetic Field Laboratory was used to provide the high magnetic fields. A dual fiber probe arrangement similar to that of the 18 T MPLE was used, and the excitation was again provided by a Ti:sapphire laser. However, the signal detection was performed using a 1m double grating spectrometer with extremely high stray light rejection, which enabled the detection to be performed via a liquid-nitrogen-cooled charge coupled device array, thus enabling us to perform parallel detection at many wavelengths.

III. RESULTS

Figure 2 shows the state-filling spectroscopy of the QD ensemble where the emission intensity of higher-energy excited-state transitions increases with excitation power. In

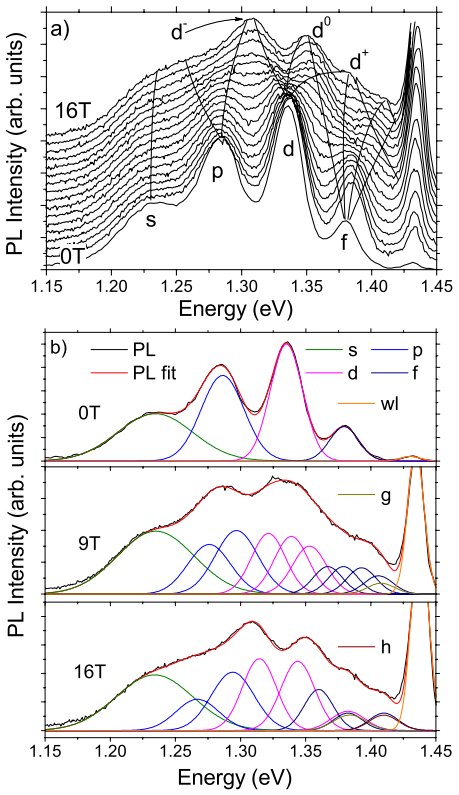

FIG. 3. (Color online) (a) Magnetophotoluminescence of the QD ensemble for an excitation power of 56 mW. The lines are a guide to the eyes showing the approximate position of the different angular-momentum channel transitions as the magnetic field increases. At 16 T, a set of resolved peaks appears which indicates that other degeneracies are obtained involving, among others, the d^-, d^0 and d^+ branches. (b) Example of multi-Gaussian fit showing how transitions with different angular momenta evolve with magnetic field to produce the observed spectrum.

total four QD peaks are resolved, which we ascribe to *s*-, *p*-, *d*-, and *f*-shell transitions in the QDs.[12] At the highest excitation power, a weak signal from the wetting layer (WL) is also observed at ~1.425 eV. It is important to note the broadening and redshift of the *s*-shell emission energy as the excitation intensity increases from 1.245 to 1.235 eV when going from 5 to 56 mW excitation. The other transitions also show this type of redshift with increasing power, although the effect is less pronounced. Below 5 mW of excitation power, the shape of the spectrum remains the same, and therefore 1.245 eV is the average emission energy of the single-exciton line for our sample.

The interpretation of the different transitions observed in the PL spectra is confirmed by MPL. Figure 3(a) shows the evolution of the high excitation emission spectrum when subjected to a perpendicular magnetic field (Faraday configuration). One observes the typical PL line splitting and crossing pattern of self-assembled QDs with increasing magnetic field. Neglecting spin effects which are masked by the inhomogeneous broadening, the *s*-shell has a degeneracy of 1 ($L=0$), the *p*-shell a degeneracy of 2 ($L=+1,-1$), the *d*-shell a degeneracy of 3 ($L=-2,0,+2$), and so on. Accordingly, the *s*-shell, with only one angular-momentum channel ($L=0$), undergoes a small diamagnetic shift toward higher energies, while excited-state emission lines undergo a Zeeman-type splitting according to their angular-momentum degeneracy.[12,24] The *p*-shell splits into two lines, one for each of its angular-momentum channels, $L^e=-1$ and $L^e=+1$, which shifts toward lower and higher energies, respectively. The *d*-shell splits into three lines and so on. The solid lines are a guide to the eyes indicating the approximate evolution of the different transition lines.

Figure 3(b) presents an example of multi-Gaussian fits to illustrate the evolution of the different transitions and how it relates to the measured PL spectrum. At 0 T, each transition is fitted with a single Gaussian peak to obtain the best possible match to the corresponding PL spectrum. Each of these lines can be viewed as the result of the superposition of one transition peak for each angular-momentum channel within the shell. Applying a magnetic field results in these peaks moving in different directions in energy, thus causing changes in the overall PL spectrum. For example, at 9 T the peaks related to each angular-momentum channel have started to separate, causing mostly a broadening of the observed transitions. This broadening is more pronounced for higher-energy shells since the higher angular momentum of the states in these shells results in larger shifts due to stronger interaction with the magnetic field. Note also that in order to keep consistent peak intensities for the *f*-shell transitions, we had to add an extra peak near the WL emission. This is consistent with an energy level, called "*g*," peeling off from the WL continuum and becoming bound into the QD as the field is increased, a phenomenon which was observed in previous work.[12] Increasing the magnetic field results in further splitting until for a specific magnetic field another set of degeneracies is obtained, giving rise to a new set of well-resolved peaks. For example, in Fig. 3(a) at 16 T the symbols d^- ($L^e=-2$), d^0 ($L^e=0$), and d^+ ($L^e=+2$) indicate the three transition peaks involving one of the three *d*-shell angular-momentum states. The corresponding fit is shown in Fig. 3(b) where the p^+ and d^- peaks are close enough in energy to produce a single well-resolved peak, and the same is true for the d^0 and f^- peaks. At the same time, d^+, f^-, and *g* form another energy shell, and also f^+ and *h* (a newly confined transition).

We estimate that, for the case shown in Fig. 3(a), the QDs are filled with an average of 14 excitons, corresponding to filled *s*, *p*, and *d* shells and partly filled *f*-shell. The *B*-field evolution observed in Fig. 3(a) therefore describes the energy shell structure of an excitonic droplet confined in a QD with associated many-body interactions. A realistic quantitative description of the results requires intensive theoretical modeling, involving atomistic modeling of bound states, blended with many-body theory. This is not presented here, and the lines shown on top of the MPL experiment in Fig. 3(a) are guides to the eyes only. The energy shell structure of a single exciton is easier to describe theoretically, and therefore it would be desirable to obtain this type of data as a stepping stone in our understanding of QD bound states. Moreover, such data could be compared with data obtained for excitonic droplets and obtain information on the magnitude of many-body interactions.

To observe the single-exciton energy shell structure, one can perform an absorption experiment where excitons are

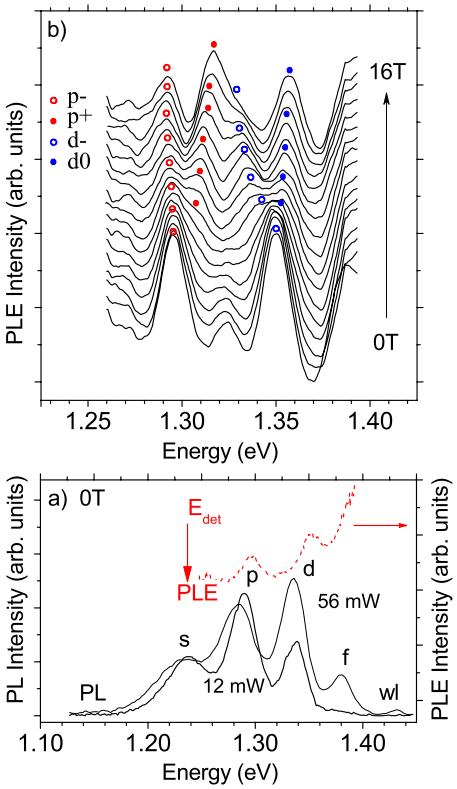

FIG. 4. (Color online) (a) Comparison of PL and PLE spectra obtained at 0 T, where the red vertical arrow indicates the PLE detection energy. (b) Evolution of the PLE spectrum with magnetic field. Open (full) circles are guide-for-the-eye symbols to illustrate the evolution of transition energies for negative (zero or positive) angular-momentum states. The detection energy is set at 1.238 eV for all PLE spectra presented, as indicated by the arrow.

absorbed in the QDs one at a time, in either the GS or excited states, and the absorption spectrum is monitored as a function of magnetic field. The difficulty resides in the very small absorption cross section of the QDs and the inhomogeneous broadening. The first difficulty means that if one uses a broadband source to illuminate the sample and compare the transmitted spectrum with the incident source spectrum, the differences will be minute and difficult to resolve. This difficulty can be overcome with proper experimental schemes,[25] but to implement those in current high-magnetic-field apparatus appears impractical. The second difficulty means that it can be difficult to resolve the different transitions in the spectrum. This can be overcome if one selects a set of QDs with similar energies. Performing PLE spectroscopy incorporates these two elements; i.e., PLE is an absorption experiment in which, after a relaxation process, one monitors the emission over a narrow energy band in the *s*-shell to obtain signal. The trade-off is that one must take into account the different possible relaxation mechanisms within the QD in the analysis. These include different relaxation pathways from excited states to ground state, as well as radiative recombination from an excited state and nonradiative recombination.

Figure 4(a) shows a comparison between PL (black solid curves) and PLE (red dashed curve) spectra obtained at zero field. The detection energy for the PLE experiments was fixed at 1.238 eV, which is just below the average single-exciton line transition energy.[26] Despite that, the most prominent PLE peaks, presumably corresponding to *p*- and *d*-shell absorptions, appear at higher energy than the *p*- and *d*-shell emission peaks. This may seem surprising for low-temperature measurements on zero-dimensional structures with high confinement energy. For quantum well (QW) structures, a significant Stokes shift is often interpreted as originating from material nonuniformity where in PL experiments carriers tend to diffuse toward regions of lower band gap, causing the PL emission to be redshifted when compared with PLE.[27] In our case, carrier transfer between QDs via tunneling or thermal excitation or diffusion process could in principle produce a similar effect. However, it has been shown using time-resolved spectroscopy that such carrier transfer does not happen at low temperatures for samples with QD densities below 1×10^{10} cm^{-2}.[28] Moreover, in samples with strong lateral coupling, the spectral features broaden considerably toward higher energies as the excitation intensity is increased.[29] This is not observed in Fig. 2. On the contrary the PL lines in our sample broaden toward lower energies. Other authors have observed QD electron to WL hole state transitions in their PLE spectra,[16] in which case one certainly expects to observe an offset between the PL and PLE peaks. However, in our case the observed energy spacing between the *p*- and *d*-shell transitions is greater than that observed in the PL, whereas for QD to WL transitions that spacing should be smaller i.e., the spacing between the *p*- and *d*-shell QD electron states only. Others have invoked phonon-assisted absorption mechanisms, but in our case the energy offset between the PL and PLE peaks is on the order of 10–20 meV, while the energy spacing between the main PLE peaks is 56 meV. Neither of these corresponds to LO phonon energies of the materials in our sample. The interpretation of the observed PLE peaks is rather consistent with the interpretation of Hawrylak *et al.*[7] who performed single-dot PLE on similar types of QDs and attributed observed resonances to interband transitions between *p*- and *d*-shell QD bound states.

The nature of the transitions observed is confirmed by magneto-PLE experiments. Figure 4(b) shows the corresponding experimental results, where in order to enhance the contrast of the different QD transitions, the second derivative of the raw data is presented. Looking at the 0 T PLE spectrum, four spectral regions of interest are identified. First, a weak doublet is observed with peak energies of 1.268 and 1.272 eV, 30–34 meV above the detection energy. This is consistent with phonon-assisted absorption in the GS of the QDs. These transitions are very weak compared to the other ones observed in our spectrum, confirming that the latter are unlikely to be related to phonon-assisted transitions. The second peak region is that located around 1.295 eV. The blueshift of this absorption peak with respect to the *p*-shell emission may suggest that it has a different origin. However, with increasing magnetic fields, this peak shifts toward lower energies (position indicated by open red circles) and progressively loses its oscillator strength. Around 5–6 T, a shoulder starts appearing on the high-energy side. This shoulder progressively increases in intensity and shifts toward higher en-

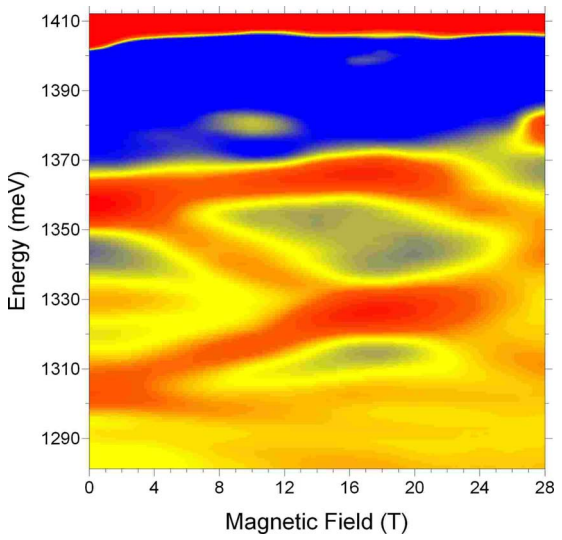

FIG. 5. (Color online) Surface plot of the magneto-PLE with detection energy of 1.245 eV. In order of increasing intensity, the emission is represented by blue, yellow, orange, and red. The p^e-p^h and d^e-d^h transitions are observed at 1305 and 1358 meV, respectively.

ergies (position indicated by filled red circles) as the intensity of the field increases. This progressive splitting is consistent with the behavior of p^- and p^+ transitions, and we therefore attribute this peak to p-shell absorption. The third peak located at 1.324 eV shows no shift with magnetic field and disappears around 8 T. The fourth peak at 1.350 eV is tentatively attributed to d-shell absorption. One can see a clear twofold splitting with the d^- component shifting toward lower energies (open blue circles) and the d^0 component slowly shifting toward higher energies (filled blue circles). According to the energy shell structure of a cylindrically symmetric QD, the d-shell absorption should split into three different components, which is not observed here. On the other hand, at 16 T the PL shows an emission peak at 1.383 eV which is the result of the crossing of the d^+ branch with the lower f and g branches. The three-way splitting of the d-shell was also observed clearly in other MPL experiments.[12,13]

More insight on the evolution of the d^+ branch was obtained from another MPLE experiment, this time setting the detection signal at 1.245 eV, and Fig. 5 presents the surface plot of the second derivative of the data. The main features of Fig. 4(b) are reproduced: a weak signal at low energies, a p-shell peak (1.297 eV) with two-way splitting, a nonshifting peak (1.330 eV) which disappears around 8 T, and a d-shell peak (1.363 eV). The features are shifted toward higher energies since the detection energy is higher and a different set of dots is probed. The main difference in Fig. 5 is that the surface plot shows indication of a three-way splitting of the d shell. In fact, one can clearly see a branch shifting toward lower energies, another branch slowly shifting toward higher energies, and the third branch is revealed when it crosses with the f^{--} branch at 10 T and produces a peak at 1.380 eV. A second crossing occurs at 17 T, 1.400 eV when the d^+ branch crosses with the lower g-shell branch. So, it appears that the oscillator strength of the d^+ branch is lower than that of the d^- and d^0 branches, and it is therefore more difficult to observe it above the background in the experiment.

IV. DISCUSSION

The intensity of the dot signal in PLE spectroscopy depends on the probability of absorption of the incident photon, the probability of electron-hole pair relaxation to the emitting s shell, and the probability of radiative recombination from there.[30] Through the first probability, the PLE intensity is thus related to the absorption spectrum of the QD transitions. The results in Fig. 2 show that for low enough excitation power, only GS emission is observed, thus confirming that relaxation to the GS occurs on a shorter time scale than excited-state radiative recombination. Moreover, for coherently strained self-assembled QD samples with direct band gap, nonradiative recombination can be neglected at low carrier densities, and therefore in the present case the PLE spectrum is in fact proportional to the absorption spectrum of the subset of QDs selected by the detection window.

To gain more insight in the observations, the results are compared to exact diagonalization calculations of the QD absorption spectrum.[31] The one-exciton Hamiltonian reads

$$H = \sum_i E_i^e c_i^+ c_i + \sum_i E_i^h h_i^+ h_i - \sum_{ijkl} V_{ijkl}^{\text{e-h}} c_i^+ h_j^+ h_k c_l, \qquad (1)$$

where c^+, c, h^+, and h are the creation-annihilation operators for electrons and holes, respectively, E^e and E^h are the electron and hole kinetic energy, and $V^{\text{e-h}}$ is the electron-hole Coulomb potential. The indices i, j, k, and l run over all QD confined states. Using Fock-Darwin states as a basis, we build the one-exciton configurations including the five lowest FD energy shells. We then build the Hamiltonian matrix related to Eq. (1) with off-diagonal elements describing the coupling between the different single-particle configurations and diagonalize it. The eigenstates and eigenenergies are denoted by $|X;i\rangle$ and E_i, respectively. The absorption spectrum is then obtained from Fermi's golden rule

$$A(\omega) = \sum_f |\langle X;f|P^+|vac\rangle|^2 \delta(\hbar\omega - E_f), \qquad (2a)$$

where

$$P^+ = \sum_{i,\sigma} c_{i\sigma}^+ h_{i-\sigma}^+ \qquad (2b)$$

is the polarization operator which generates electron-hole pairs with opposite spins.

Figure 6 shows the results of the calculation where the size of the circles is proportional to the absorption (oscillator) strength and the center of the circles indicate the transition energy. Note that only relative energies should be considered, as the parameters were not adjusted to fit the absolute emission energies. At zero fields, one observes three main transitions: the s-, p-, and d-shell-derived transitions at 35, 100, and 165 meV, respectively. The s-shell transition simply undergoes a small diamagnetic shift as the field is increased, with no splitting or changes in oscillator strength.

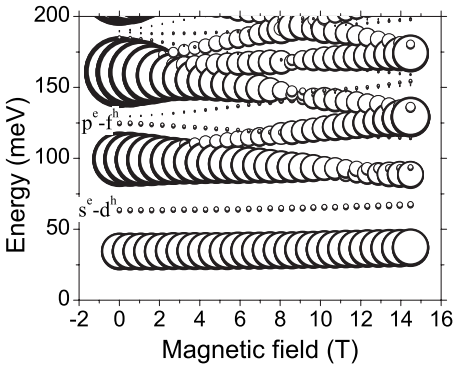

FIG. 6. Calculated absorption spectrum of quantum dot states in magnetic field. The calculations were performed using electron and hole masses and confinement energies of $0.05m_0$ and $0.25m_0$ and 49.5 and 9.9 meV, respectively. The size of the circles is proportional to the oscillator strength.

The next transition is the *p*-shell transition at ~100 meV. The calculation predicts a progressive redshift of this transition along with decreasing oscillator strength as the field increases. At the same time, a second transition progressively emerges on the high-energy side, with increasing blueshift and oscillator strength as the field increases. This evolution is in excellent agreement with what is observed experimentally. The *d*-shell transition is predicted to be the strongest one at zero field, and again the main peak is predicted to undergo a redshift along with a decrease in oscillator strength as the field increases. The d^0 and d^+ branches progressively increase their oscillator strength as the field increases, where the difficulty to resolve the d^+ branch in PLE measurements is explained by its smallest oscillator strength at low fields. To understand the origin of this weak oscillator strength for the upper branches, it is useful to think in terms of Jacobi coordinates.[7] In such coordinates, the *d*-shell is composed of one coherent bright state and two dark states. With increasing magnetic field the bright state shifts to lower energies while it loses oscillator strength due to admixture with dark states. By the same token, dark states slowly increase their oscillator strength and start shifting toward higher energies. By the time the d^+ transition should have picked up enough oscillator strength to be visible, it has shifted to higher energies where it is superimposed on a strong absorption background from the wetting layer, meaning that this state progressively becomes unbound which decreases its oscillator strength. Hence, one can resolve the d^+ branch in Fig. 5 only when it crosses with the lowest *f* and *g* branches to create a stronger "combined" transition.

By comparing the calculation results with the data of Figs. 4(b) and 5, we also obtain clues as to the origin of the weaker transitions observed in the PLE experiments. We find that the weak PLE signal at low energies [~1.27 eV in Fig. 4(b)] may result from a transition between an electron in the *s* shell and a hole in a *d*-shell zero-angular-momentum state. This may be superimposed on peaks originating from a three-particle absorption process in which an electron-hole pair is created in the QD GS at the same time as a phonon is created in the lattice. Approximately midway between the energy of the *p*- and *d*-shell transitions, another weak resonance is observed due to *p*-electron to *f*-hole transitions. There are in fact two such transitions: one from the p^+ to f^+ and one from p^- to f^- branches, and consequently these transitions will split with increasing fields according to a pattern close to the *p*-shell splitting. This explains the PLE signal at 1.324 eV [Fig. 4(b)] and 1.330 eV (Fig. 5), with the feature almost disappearing in the background as the transitions are split by the field. However, a faint trace shifting toward higher energies of the p^+-f^+ transition seem to be present in Fig. 5, with a crossing with the d^- branch obtained around 9–10 T, as predicted by theory.

The close correspondence of the experimental results with the theoretical calculations leads us to conclude that all of the observed transitions in our PLE spectrum can be attributed to transitions between QD bound states. Knowing this, the origin of the blueshift of the absorption peaks with respect to corresponding emission peaks is attributed to extra Coulomb interaction and exchange and correlation energies of the excitonic droplet probed in PL as opposed to the single QD exciton probed in PLE. This is the same interpretation put forward by Warburton *et al.*[32] who explained the shift of the absorption peaks in their experiments on charged QDs as originating from Coulomb interactions.

As an example, let us consider the case of Fig. 4(a) where the 12 mW PL *d*-shell emission energy is compared to the PLE *d*-shell absorption at zero field. The PL spectrum in that case has filled *s*- and *p*-shells and a less than half filled *d*-shell, as can be inferred by comparison with the PL taken at an excitation of 56 mW. Therefore, we estimate that the QD is filled with eight QD excitons on average. The *d*-shell PL emission energy is then given by

$$\mu_8 = E_{\text{tot}}^{8X,\text{GS}} - E_{\text{tot}}^{7X,\text{GS}}, \tag{3}$$

where μ_8 is the energy necessary to add or remove the eighth QD exciton from the QD droplet and $E_{\text{tot}}^{nX,\text{GS}}$ refers to the total energy of an *n*-exciton droplet confined in a QD in its ground-state configuration. For an 8*X* and a 7*X* QD-exciton droplet, the total energy can be written as

$$E_{\text{tot}}^{8X,\text{GS}} = E_{\text{tot}}^{6X,\text{GS}} + 2K^{1X,d} - 2V_{\text{direct}}^{1X,d} - 2V_{\text{exch}}^{1X,d\text{-}6X\text{GS}} - V_{\text{corr}}^{2X,d\ \text{singlet}}, \tag{4a}$$

$$E_{\text{tot}}^{7X,\text{GS}} = E_{\text{tot}}^{6X,\text{GS}} + K^{1X,d} - V_{\text{direct}}^{1X,d} - V_{\text{exch}}^{1X,d\text{-}6X\text{GS}} - V_{\text{corr}}^{1X,d}, \tag{4b}$$

where $K^{1X,d}$ is the kinetic energy of one exciton in the *d* shell, $V_{\text{direct}}^{1X,d}$ is the direct Coulomb attraction energy of an exciton in the *d*-shell, $V_{\text{exch}}^{1X,d\text{-}6X\text{GS}}$ is the exchange energy of an extra exciton in the *d*-shell with a core of six excitons in its ground-state configuration, $V_{\text{corr}}^{1X,d}$ is the correlation energy of a single exciton populating a *d* shell, and $V_{\text{corr}}^{2X,d\ \text{singlet}}$ is the correlation energy of a biexciton populating a *d* shell in its singlet configuration (we find numerically that this is the ground-state configuration for an 8*X* droplet). Note that the configuration of the filled core shells is considered "frozen" in the calculation of the correlation energies since *d*-shell excitons can easily be rearranged to produce same-energy configurations, which is not possible for core-shell excitons. In Eq. (4) we have assumed the electron-electron (e-e) and

hole-hole (h-h) repulsion energies to be equal to the e-h attraction, an approximation which we expect to be reasonable for a flat disk QD. The resulting photon energy is given by

$$\mu_8 = K^{1X,d} - V_{\text{direct}}^{1X,d} - V_{\text{exch}}^{1X,d\text{-}6X\text{GS}} - (V_{\text{corr}}^{2X,d\ \text{singlet}} - V_{\text{corr}}^{1X,d}). \tag{5}$$

Similarly, we can calculate the energy of a photon absorbed in the *d*-shell of an empty dot as follows:

$$E_{\text{PLE}}^{d,1X} = K^{1X,d} - V_{\text{direct}}^{1X,d} - V_{\text{corr}}^{1X,d}. \tag{6}$$

Finally, the difference between the last two quantities should be equal to the blueshift of the PLE *d*-shell with respect to the PL *d*-shell,

$$\Delta E_{\text{PLE-PL}} = V_{\text{exch}}^{1X,d\text{-}6X\text{GS}} + V_{\text{corr}}^{2X,d\ \text{singlet}} - 2V_{\text{corr}}^{1X,d} \approx V_{\text{exch}}^{1X,d\text{-}6X\text{GS}}. \tag{7}$$

In the expression on the right-hand side of Eq. (7), the correlation energy of a QD biexciton on the *d*-shell is set to be approximately equal to twice the correlation energy of a single QD exciton on the *d*-shell. This is justified by our numerical calculations which show that $V_{\text{corr}}^{2X,d\ \text{singlet}} \approx 2.005 V_{\text{corr}}^{1X,d}$. Thus, the blueshift of the PLE *d*-shell absorption with respect to the *d*-shell emission can be interpreted as a measure of the difference in total exchange energy in the excitonic droplet when an exciton is added in the *d*-shell. Comparing the peak positions of the respective *d*-shells in Fig. 4(a), we find $V_{\text{exch}}^{1X,d\text{-}6X\text{GS}} \approx 10$ meV. Note that this underestimates the real value since the correct comparison should be made when the PLE detection energy is set as the peak of the single-exciton *s*-shell emission. In the case of Fig. 4(a), the PLE detection energy was set below the *s*-shell peak by about 7 meV, and therefore the relevant blueshift is larger than the value quoted above. Moreover, the above discussion neglects charge fluctuations which occur in PL experiments. A time-average population of eight excitons means that the QD population fluctuates between six and ten excitons most of the time, and also the net charge will oscillate between positive and negative. Although this will cause added uncertainty, the deviations from the mean peak position due to these fluctuations will sometimes be positive and sometimes negative, thus causing extra broadening but more or less preserving the same peak position. In the end, the magnitude of the exchange energy obtained is in the range one would expect from a theoretical standpoint, which supports the attribution of the observed offset between corresponding PL and PLE transitions to many-body effects.

V. SUMMARY

We have performed magnetoabsorption (MPLE) spectroscopy of self-assembled quantum dot ensemble and have been able to establish that observed resonances originate from QD bound-state transitions; in particular, two stronger transitions are attributed to p^e-p^h and d^e-d^h. Due to the selective nature of the PLE experiment, the inhomogeneous broadening is reduced as compared to PL experiments, and this allowed us to resolve some weaker transitions as well, such as s^e-d^h and p^e-f^h. A theoretical model based on exact diagonalization showed good agreement with experiment, as it reproduced the transitions observed in the experiment as well as their relative strength. Moreover, the model correctly predicts the evolution of the different transitions with magnetic field, including their energy shift and change in oscillator strength, thus giving us a high level of confidence in the correctness of the model and our interpretation of the experimental results. Taking advantage of this knowledge, we interpret the blueshift of the PLE resonances with respect to corresponding PL resonances as a manifestation of many-body effects. We have shown that for the case of the *d*-shell PL emission, the energy difference between the PL and the absorption (PLE) peaks for the case of a QD filled with eight excitons gives a direct measure of the increase in exchange energy when one adds the eighth exciton in a QD already filled with seven excitons. We obtain a lower bound value of 10 meV for the type of QDs in our sample.

ACKNOWLEDGMENTS

The authors would like to acknowledge the help of M. Guy Parent for TEM sample preparation. S.A. would like to acknowledge the Institute for the Promotion of Teaching Science and Technology (IPST Thailand) for its support. A.B. would like to acknowledge the support of the EC Grant No. MTKD-CT-2005-029671. M.V. would like to acknowledge NSERC for its support. S.J.C. acknowledges the National Science Council of Taiwan for financial support under Contract No. NSC-93-2112-M-009-020 and the Institute for Microstructural Sciences for hospitality. M.P. would like to acknowledge EC Grant No. RITA-CT-2003-505474 and NRC (Canada)-CNRS (France) CRP.

[1] M. Sugawara, N. Hatori, M. Ishida, H. Ebe, Y. Arakawa, T. Akiyama, K. Otsubo, T. Yamamoto, and Y. Nakata, J. Phys. D **38**, 2126 (2005).

[2] S. K. Ray, T. L. Choi, K. M. Groom, H. Y. Liu, M. Hopkinson, and R. A. Hogg, IEEE Photon. Technol. Lett. **19**, 109 (2007).

[3] T. Akiyama, M. Ekawa, M. Sugawara, K. Kawaguchi, H. Sudo, A. Kuramata, H. Ebe, and Y. Arakawa, IEEE Photon. Technol. Lett. **17**, 1614 (2005).

[4] Z. Yuan, B. E. Kardynal, R. M. Stevenson, A. J. Shields, C. J. Lobo, K. Cooper, N. S. Beattie, D. A. Ritchie, and M. Pepper, Science **295**, 102 (2002).

[5] X. Li, Y. Wu, D. Steel, D. Gammon, T. H. Stievater, D. S. Katzer, D. Park, C. Piermarocchi, and L. J. Sham, Science **301**, 809 (2003).

[6] M. Kroutvar, Y. Ducommun, D. Heiss, M. Bichler, D. Schuh, G. Abstreiter, and J. J. Finley, Nature (London) **432**, 81 (2004).

[7] P. Hawrylak, G. A. Narvaez, M. Bayer, and A. Forchel, Phys. Rev. Lett. **85**, 389 (2000).

[8] V. Fock, Z. Phys. **47**, 446 (1928); C. G. Darwin, Proc. Cambridge Philos. Soc. **27**, 86 (1931).
[9] T. Fujisawa, D. G. Austing, Y. Tokura, Y. Hirayama, and S. Tarucha, Nature (London) **419**, 278 (2002); C. Gould, P. Hawrylak, A. S. Sachrajda, Y. Feng, and Z. Wasilewski, Physica B **256-258**, 141 (1998).
[10] H. Drexler, D. Leonard, W. Hansen, J. P. Kotthaus, and P. M. Petroff, Phys. Rev. Lett. **73**, 2252 (1994).
[11] S. Raymond, P. Hawrylak, C. Gould, S. Fafard, A. Sachrajda, M. Potemski, A. Wojs, S. Charbonneau, D. Leonard, P. M. Petroff, and J. L. Merz, Solid State Commun. **101**, 883 (1997); P. P. Paskov, P. O. Holtz, B. Monemar, J. M. Garcia, W. V. Schoenfeld, and P. M. Petroff, Phys. Rev. B **62**, 7344 (2000); R. Rinaldi, P. V. Giugno, R. Cingolani, H. Lipsanen, M. Sopanen, J. Tulkki, and J. Ahopelto, Phys. Rev. Lett. **77**, 342 (1996); S. Ménard *et al.*, J. Vac. Sci. Technol. B **20**, 1501 (2002).
[12] S. Raymond, S. Studenikin, A. Sachrajda, Z. Wasilewski, S. J. Cheng, W. Sheng, P. Hawrylak, A. Babinski, M. Potemski, G. Ortner, and M. Bayer, Phys. Rev. Lett. **92**, 187402 (2004).
[13] A. Babinski, M. Potemski, S. Raymond, J. Lapointe, and Z. R. Wasilewski, Phys. Rev. B **74**, 155301 (2006).
[14] Even for resonant excitation and low excitation powers, D. Morris *et al.* found that the rise time of the GS PL is 35 ps or shorter; see D. Morris, N. Perret, and S. Fafard, Appl. Phys. Lett. **75**, 3593 (1999).
[15] M. Notomi, T. Furuta, H. Kamada, J. Temmyo, and T. Tamamura, Phys. Rev. B **53**, 15743 (1996).
[16] S. Fafard, D. Leonard, J. L. Merz, and P. M. Petroff, Appl. Phys. Lett. **65**, 1388 (1994); R. Oulton, J. J. Finley, A. I. Tartakovskii, D. J. Mowbray, M. S. Skolnick, M. Hopkinson, A. Vasanelli, R. Ferreira, and G. Bastard, Phys. Rev. B **68**, 235301 (2003).
[17] L. R. Wilson, D. J. Mowbray, M. S. Skolnick, M. Morifuji, M. J. Steer, I. A. Larkin, and M. Hopkinson, Phys. Rev. B **57**, R2073 (1998).
[18] A. Babinski, S. Awirothananon, S. Raymond, S. Studenikin, P. Hawrylak, S.-J. Cheng, W. Sheng, Z. Wasilewski, M. Potemski, and A. Sachrajda, Physica E (Amsterdam) **22**, 603 (2004).
[19] Y. Toda and Y. Arakawa, IEEE J. Sel. Top. Quantum Electron. **6**, 528 (2000).
[20] S. Kuroda, N. Ihto, Y. Terai, K. Takita, T. Okuno, M. Nomura, and Y. Masumoto, J. Alloys Compd. **371**, 31 (2004).
[21] A. Zrenner, F. Findeis, M. Baier, M. Bichler and G. Abstreiter, Physica B: Condens. Matter **298**, 239 (2001).
[22] Z. R. Wasilewski, S. Fafard, and J. P. McCaffrey, J. Cryst. Growth **201-202**, 1131 (1999).
[23] S. Fafard and C. Nì. Allen, Appl. Phys. Lett. **75**, 2374 (1999).
[24] A. Wojs, P. Hawrylak, S. Fafard, and L. Jacak, Phys. Rev. B **54**, 5604 (1996); A. Wojs and P. Hawrylak, *ibid.* **53**, 10841 (1996).
[25] C. S. Dürr, R. J. Warbuton, K. Karrai, J. P. Kotthaus, G. Medeiros-Ribeiro, and P. M. Petroff, Physica E (Amsterdam) **2**, 23 (1998).
[26] We have independently measured the *s*-shell diamagnetic shift to be 2 meV over the range of magnetic fields investigated. Formally, the detection energy should have been changed at every magnetic field to account for this effect. In view of the small magnitude of this shift compared to *p*- and *d*-shell shifts, this was neglected in the experiment and the detection energy was kept constant. This produces a small error on the slope of the shifts observed in Fig. 4(b) where transitions should shift +2 meV/T faster than observed. This does not affect results at 0 T.
[27] A. Polimeni, A. Patanè, M. Grassi Alessi, M. Capizzi, F. Martelli, A. Bosacchi, and S. Franchi, Phys. Rev. B **54**, 16389 (1996).
[28] K. L. Silverman, R. P. Mirin, and S. T. Cundiff, Phys. Rev. B **70**, 205310 (2004).
[29] S. Lan, K. Akahane, H.-Z. Song, Y. Okada, M. Kawabe, T. Nishimura, and O. Wada, Phys. Rev. B **61**(24), 16847 (2000).
[30] P. Yu and M. Cardona, *Fundamentals of Semiconductors* (Springer, Berlin, 1999), p. 357.
[31] P. Hawrylak, Phys. Rev. B **60**, 5597 (1999).
[32] R. J. Warburton, C. S. Dürr, K. Karrai, J. P. Kotthaus, G. Medeiros-Ribeiro, and P. M. Petroff, Phys. Rev. Lett. **79**, 5282 (1997).